May 1996

Epitaxial growth of Co_3O_3 on CoO(100)

G.A. Carson
University of Nebraska - Lincoln

M.H. Nassir
University of Nebraska - Lincoln

Marjorie Langell
University of Nebraska - Lincoln, mlangell1@unl.edu

Epitaxial growth of Co_3O_4 on CoO(100)

G. A. Carson, M. H. Nassir, and M. A. Langell
Department of Chemistry, University of Nebraska–Lincoln, Lincoln, Nebraska 68588–0304

(Received 17 October 1995; accepted 12 February 1996)

Under mildly oxidizing ultrahigh vacuum conditions, it is possible to form on top of CoO(100) single crystal substrates, thin films that have higher oxygen content but that preserve the overall symmetry of the CoO(100) low-energy electron diffraction pattern. X-ray photoelectron spectroscopy (XPS) and high-resolution electron-energy-loss spectroscopy (HREELS) data indicate that the epitaxial film grown on CoO(100) at 625 K and 5×10^{-7} Torr is Co_3O_4-like in both oxygen content and XP/HREEL spectroscopic characteristics. Both materials are closest packed in lattice oxygen, with the mismatch of bulk O^{2-}–O^{2-} distances of approximately 5%. However, the Co_3O_4 is only able to grow to a thickness of approximately 5 Å before the oxidation process halts. It is proposed that the orientation of Co_3O_4 that forms most readily on the CoO(100) surface does not present a thermodynamically stable orientation of the bulk Co_3O_4 substrate but is that which grows under the constraint of the best CoO(100)/Co_3O_4 epitaxial arrangement. While the mismatch in lattice parameters may in part be to blame for the limitation of higher oxide thickness, thicker oxide films have been grown under conditions with significantly larger mismatch.

I. INTRODUCTION

CoO is a rocksalt $3d$ transition metal monoxide with interesting electronic and chemical properties. The material is closest packed in O^{2-}, forming a face-centered cubic arrangement with Co^{2+}-filled octahedral sites. The valence band is primarily comprised of cobalt $3d$ orbitals with some admixture from their neighboring oxygen $2p$.[1] Despite the unfilled character of the valence band, the bonding is localized and the material is a charge transfer insulator with a band gap of approximately 6 eV.[2] It is antiferromagnetic below temperatures of 289 K.[3] The thermodynamically stable surface of CoO is formed along the (100) nonpolar orientation in which cations and anions most favorably balance out electrostatic interactions in interpenetrating square arrays.

Chemically, the metal monoxides find use as partial oxidation catalysts[4,5] and as gas sensors.[6] Not coincidental to these applications is the easy accessibility of a second oxidation state of cobalt, Co^{3+}. More highly oxidized cobalt compounds are well known in the solid state. In particular Co_3O_4 is thermodynamically stable under a wide range of substrate temperature and oxygen partial pressure conditions, and may form[7] on the CoO surface under oxidizing reaction conditions. The oxygen lattice structure of the bulk Co_3O_4 is similar to that of CoO with the closest O^{2-} distances matching to within 5%.[8] However Co_3O_4 possesses both Co^{3+} and Co^{2+} cations, which are distributed among the fcc octahedral and tetrahedral holes in the normal spinel structure.

In this article, we present x-ray photoelectron spectroscopy (XPS), and high-resolution electron-energy-loss spectroscopy (HREELS) data for both the stoichiometric Co(100) surface, and for the epitaxially grown, thin film of Co_3O_4. The O $1s$ and Co $2p$ XPS regions are shown as a function of oxygen exposure, and thickness calculations of the Co_3O_4 overlayer are presented along with a discussion of these phenomena.

II. EXPERIMENT

The CoO(100) single crystal, approximately $0.5\times1\times0.2$ cm^3 in size, was obtained from the Atomergic Chemetals Corp. and was grown by the flame fusion method. The crystal surface was oriented to within 1° of the (100) plane by Laue back diffraction and polished with successively finer grades of alumina to 0.03 μm alumina particle size. The crystal was then washed in trichloroethylene, and ultrasonicated in acetone and in methanol. The substrate was placed on a stainless steel backing plate and was held in place by tantalum wires which were placed across the sample edges and spot welded to the backing plate. The mounted sample was then suspended between two tantalum wires and placed between two heating posts to which the tantalum wires were spot welded. Substrate heating was achieved by direct resistive heating of the tantalum wires. The temperature was measured with a Chromel–Alumel thermocouple which had been attached to the backing plate.

The CoO(100) surface was cleaned by repeated cycles of sputtering with Ar^+ (3×10^{-5} Torr, 2 keV, 3μA/cm^2 for 15 min), annealing in oxygen (5×10^{-7} Torr, 523 K, for 15 min), and annealing in vacuum ($\leqslant3\times10^{-10}$ Torr, 523 K, for 15 min) until no impurities could be detected by Auger electron spectroscopy. The XPS data were collected at room temperature using a Physical Electronics (Φ) 15-255G double pass cylindrical mirror analyzer. The XPS photoelectrons were generated using Mg $K\alpha$ radiation ($h\nu=1253.6$ eV) with electron energy analysis done in the constant energy mode with a bandpass of 50 eV. The charging effects in the XPS spectra were compensated for by assigning a binding energy of 529.4 eV to the lattice O $1s$ peak and of 780.5 eV to the CoO Co $2p_{3/2}$ peak.

HREELS data were taken in the specular mode at 60° relative to the surface normal using a single pass 127° sector electron energy analyzer.[9] The HREELS data were taken

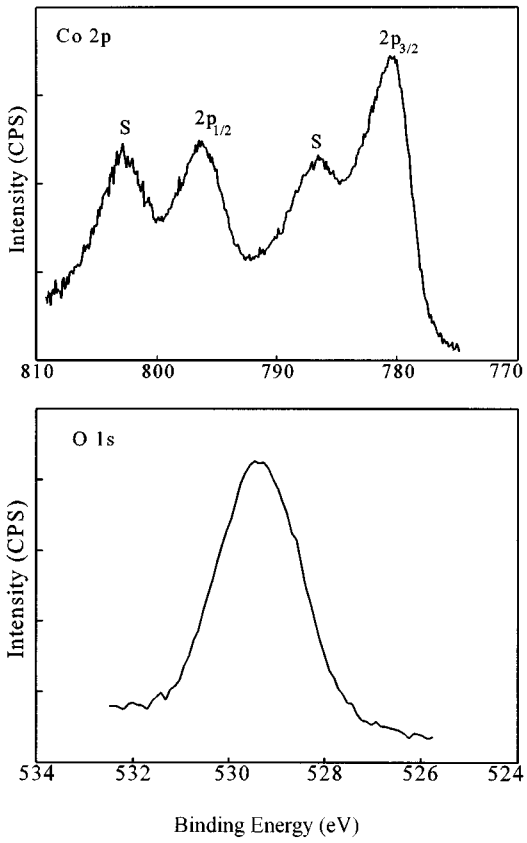

FIG. 1. O 1*s* and Co 2*p* XP spectra for stoichiometric CoO(100).

with a primary beam energy of 3.2 eV, with a resolution of 8.5 meV as measured by the full width at half-maximum of the elastic peak. Charging at the sample surface during the measurements was a problem; thus the HREELS data were collected at a substrate temperature of 500 K, an approach which was used previously with success.[10] No change in the surface composition was detected as a result of HREELS acquisition at this substrate temperature.

III. RESULTS AND DISCUSSION

XP spectra for the stoichiometric CoO(100) surface are shown in Fig. 1 and a typical HREEL spectrum is given in Fig. 2. Surface stoichiometry was confirmed by the XPS O $1s$/Co $2p_{1/2}$ intensity ratio as well as the Co $2p_{1/2}$ satellite to Co $2p_{1/2}$ main peak intensity ratio (Table I). The Co $2p$ spectrum yields a Co $2p_{3/2}$ peak at 780.5 eV while the Co $2p_{1/2}$ peak occurs at 796.4 eV with the corresponding satellites at 787.1 and 803.0 eV, respectively. Among cobalt metal and its oxides, the very intense satellite structure is specific to CoO and results from the charge-transfer band structure characteristic of the late $3d$ transition metal monoxides. The CoO valence band is primarily comprised of cobalt $3d$ orbitals. However, a significant admixture of oxygen $2p$ leads to a hybridized description of the valence band:

$$\Psi_{vb} = \alpha 3d^7 + \beta 3d^8\underline{L} + \gamma 3d^9\underline{L}^2,$$

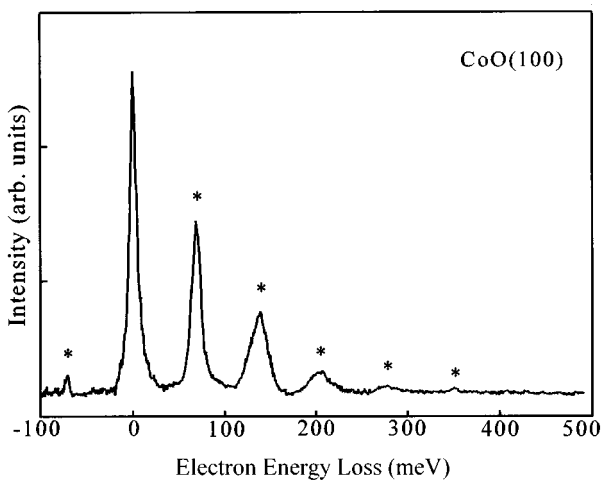

FIG. 2. HREEL Fuchs–Kliewer phonon spectrum of stoichiometric CoO(100) at a primary beam energy of 3.2 eV.

where $\underline{L}$ represents a hole in the oxygen $2p$ band. Due to the significant admixture of oxygen orbitals, photoexcitation from cobalt $2p$ core levels has a high probability of creation of both $2p^5 3d^7$ and $2p^5 3d^8\underline{L}$ final states. Studies of the resonant behavior of the satellite structure[2] indicate that the lower binding energy $2p_{3/2,1/2}$ features are associated with the $2p^5 3d^8\underline{L}$ state and the satellite peaks with the $2p^5 3d^7$ state. Co $2p_{1/2}$ satellite to main peak intensity ratios of $\sim$0.9 are characteristic of the cubic cobalt monoxide;[13] values of $\sim$0.3 have been measured for Co_3O_4.[13]

The O $1s$ peak due to lattice oxygen in CoO(100) is assigned a value of 529.4 eV as an internal binding energy calibration. Previous studies have shown that the lattice O $1s$ binding energy for transition metal monoxides is relatively insensitive to changes in near-surface stoichiometry.[14] A value of 0.41 was obtained for the XPS O $1s$/Co $2p$ intensity ratio, using the entire Co $2p_{1/2}$ (satellite plus main peaks) region, and this value is within error of 0.45 reported in the literature for CoO powders.[11] No other peaks are visible in the O $1s$ region.

The HREELS Fuchs–Kliewer phonon spectrum of stoichiometric CoO(100) is shown in Fig. 2. The CoO phonon spectrum comprises a single fundamental loss at 69.4 meV with multiple loss peaks at integral values of the single loss energy. The loss peaks decrease in intensity in a Poisson distribution,[15] indicating that the phonons behave harmonically. The Fuchs–Kliewer phonons are surface analogs of transverse optical bulk modes and thus their energy can be estimated by application of dielectric theory.[16,17] Using optical and dielectric CoO data available in the literature,[18–20] we have previously calculated[15] the fundamental phonon loss energy to be 69.5 meV, in excellent agreement with the present results. The spectrum in Fig. 2 also shows a phonon gain to the high energy side of the elastic peak due to the thermal population of phonons. In order to overcome problems with charging, HREEL spectra were acquired at a substrate temperature of 500 K. The gain to single phonon intensity ratio is in agreement with that anticipated from a

TABLE I. XPS binding energy and intensity data.

Sample	Co $2p_{3/2}$ (eV)	Satellite (eV)	Co $2p_{1/2}$ (eV)	Satellite (eV)	O $1s$[a] (eV)	Intensity ratio O $1s$/Co $2p_{1/2}$	Intensity ratio Co $2p_{1/2}$ Sat./Main
CoO(100) (this work)	780.5	787.1	796.4	803.0	529.4	0.41	0.77
Co_3O_4 (this work)	779.6 780.5	787.9	N.R.[b] 796.2	803.8	529.4 531.2	0.56	0.41
CoO[c]	780.5	786.4	796.3	803.0	529.6 531.2	0.45	0.9
Co_3O_4[c]	779.6 780.7	789.5	794.5 796.0	804.5	529.5 530.8	0.59	0.32

[a]O $1s$ lattice oxygen set to 529.4 eV.
[b]N.R.—not resolved.
[c]References 11–13.

Boltzmann population of the 69.4 meV Fuchs–Kliewer phonon at 500 K.

The stoichiometric CoO(100) sample was heated in oxygen (5×10^{-7} Torr O_2, at 625 K) for increasing lengths of time. Figure 3 shows the Co $2p$ and O $1s$ XP spectra for the series of oxygen exposures. The appearance of a second oxygen component at 531.2 eV is evident in the O $1s$ data after 30 min and the feature continues to increase slowly in intensity to saturate after approximately 300 min. The 531.2 eV peak has previously been detected in a number of studies involving air- or O_2-exposed CoO,[12,21] Co_3O_4 powders,[21–23] and oxidized Co_3O_4 thin films.[24–26] Absent in stoichiometric CoO O $1s$ XPS, the 531.2 eV species has been attributed to nonstoichiometric near-surface oxygen,[26] a more specific

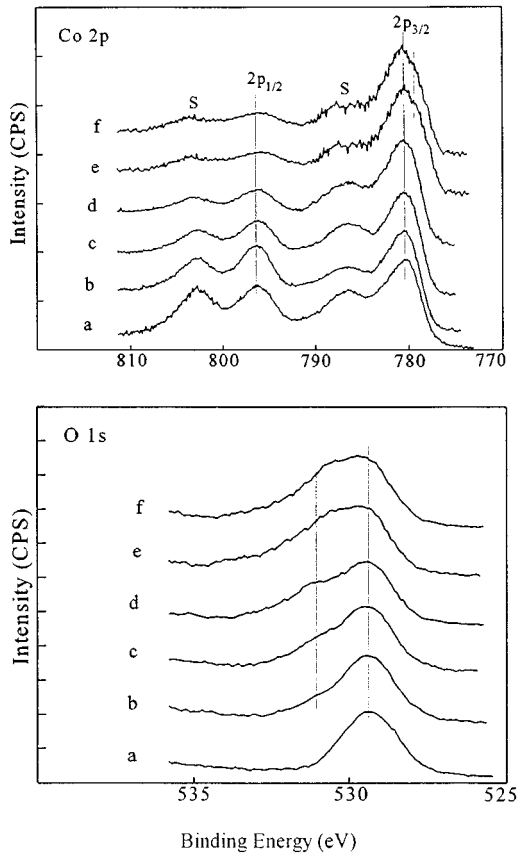

FIG. 3. X-ray photoelectron O $1s$ and Co $2p$ spectra as a function of O_2 exposure at 625 K for (a) 0 min; (b) 30 min; (c) 60 min; (d) 180 min; (e) 300 min; and (f) 360 min.

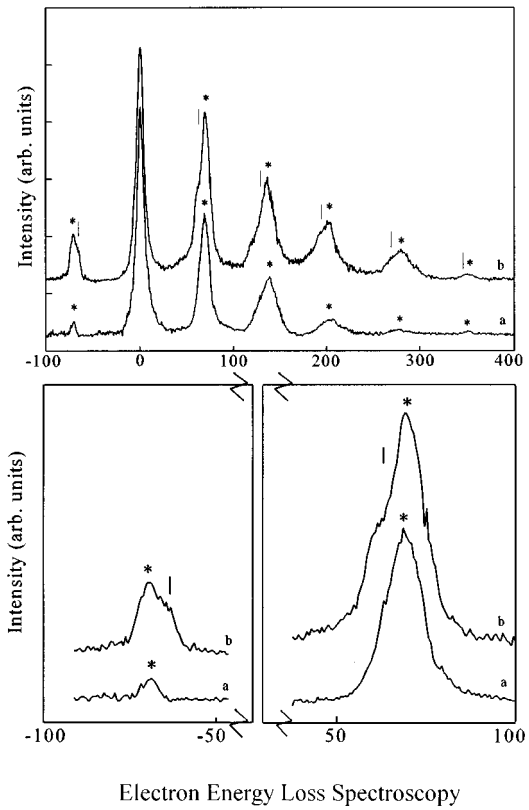

FIG. 4. HREEL Fuchs–Kliewer phonon spectrum of (a) CoO(100) and (b) oxidized CoO(100)–Co_3O_4. Top panel: full scan. Bottom panel: expanded range for single gain and loss peaks showing new phonon peak to lower gain/loss energy. Asterisks mark CoO phonon structure.

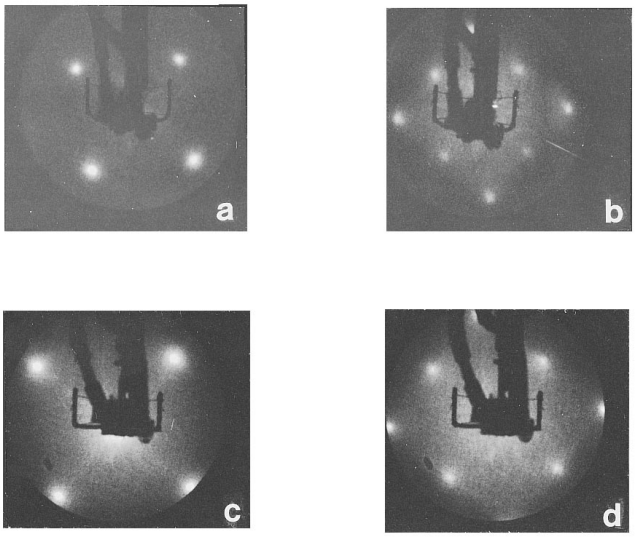

FIG. 5. LEED for CoO(100) stoichiometric surface at (a) 65 eV and (b) 85 eV, and for the oxidized CoO(100)–Co_3O_4 epitaxy at (c) 60 eV and (d) 82 eV.

near-surface O^-,[10] surface hydroxylation,[27] and $Co(OH)_2$-like thin film formation.[22,28]

HREELS of the oxidized CoO(100) surface (Fig. 4) shows no indication of electron loss to hydroxyl stretching modes (≈450 meV) and thus OH-containing species can be discounted as the source of the 531.2 eV O 1*s* peak. Depending upon the surface pretreatment conditions, the intensity of the 531.2 eV peak can rival that of the 529.4 eV O^{2-} lattice peak from the CoO substrate (Fig. 3, Refs. 12 and 26), precluding the assignment to a surface adsorbate. Additionally, angle-resolved XPS[22] has previously shown that the 531.2 eV species is distributed throughout the near-surface region. We, therefore, conclude that the 531.2 eV peak is characteristic of the oxidized CoO(100) surface and is not due to surface contamination or small quantities of defect oxide resulting from ill-formed oxide overlayers.

The top panel of Fig. 3 shows the Co 2*p* XPS spectral region as a function of oxygen exposure. Changes in the spectra correlate well with the oxidation of stoichiometric CoO(100) [Fig. 3(a)] to Co_3O_4 [Fig. 3(f)]. Co 2*p* peaks broaden due to the formation of an additional cobalt oxidation state (Co^{2+}/Co^{3+}) and eventually a double Co $2p_{3/2}$ photoelectron structure is obtained, with binding energies of 779.6 and 780.5 eV, as has been previously obtained for bulk Co_3O_4 samples. It is not possible to resolve the two individual Co $2p_{1/2}$ components. However, the peak has clearly broadened with oxygen exposure. The Co 2*p* satellite intensities also decrease substantially and approach satellite/main peak intensity ratios observed for bulk Co_3O_4. The XPS data are summarized in Table I for CoO(100) and oxidized CoO(100) after saturation to 5×10^{-7} Torr O_2 at 625 K (300 min), as well as relevant CoO and Co_3O_4 literature data. The oxidized CoO(100) surface yields XPS data consistent with the formation of a CoO(100)–Co_3O_4 thin film, although satellite intensities and peak positions indicate the oxidation to

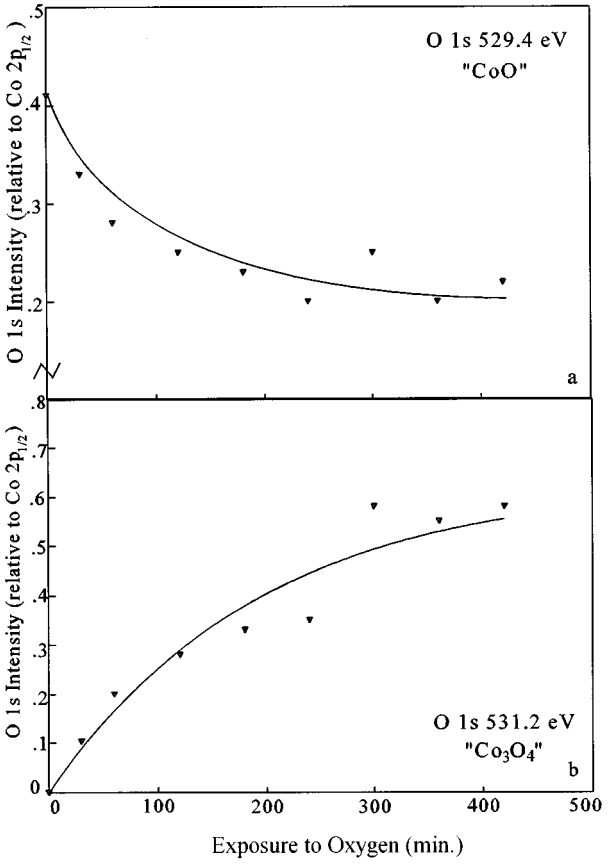

FIG. 6. CoO(100) O 1*s* XPS intensity as a function of O_2 exposure for (a) the 529.4 eV peak and (b) and 531.2 eV peak. Oxygen intensities are reported relative to that of Co $2p_{1/2}$. The solid line represents a fit to Frank–Van der Merwe layer-by-layer growth (after Ref. 29).

Co_3O_4 is not complete within the sampling depth of the XPS experiment.

The HREELS data shown in Fig. 4 corroborate the presence of a new extended oxide phase on the rocksalt CoO(100) substrate. The oxidized CoO(100) spectrum now shows two fundamental Fuchs–Kliewer phonon losses, at 59.8 and 69.8 meV, with multiple loss peaks at integral values of both fundamental phonon losses. The 59.8 meV feature has previously been associated with the formation of Co_3O_4 on CoO(100).[7] The spinel structure of Co_3O_4 is lower symmetry than that of the rocksalt CoO lattice and the 69.8 meV feature could potentially represent overlapping Co_3O_4 and CoO phonon losses. However, the HREEL spectrum of Co_3O_4 has not yet been obtained independent of a CoO(100) substrate and the contribution of Co_3O_4 to the 69.8 meV phonon structure cannot at this point be ascertained.

During oxidation, the low-energy electron diffraction (LEED) pattern obtained from the cobalt oxide surface retains the CoO(100) two-dimensional symmetry and quality, as shown for LEED from representative CoO(100) and CoO–Co_3O_4 surfaces in Fig. 5. Thus the Co_3O_4 thin film must form in close epitaxy with the underlying CoO(100) substrate. Other than a slight streaking along ⟨010⟩ and ⟨001⟩ directions [Figs. 5(c) and 5(d)], no new diffraction features

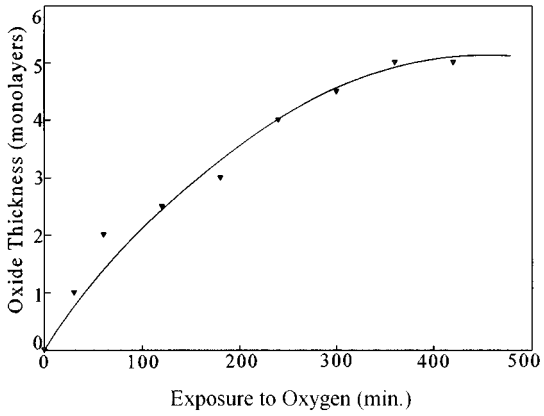

FIG. 7. Thickness of Co_3O_4 layer as a function of oxygen exposure. Thickness calculations are described in the text.

are observed at any point in the oxidation process and both diffuse background intensity and sharpness of the (1×1) diffraction features remain comparable. Sample charging made LEED problematic at 300 K and diffraction patterns could generally not be obtained below about 200 eV at this temperature. The data in Fig. 5 were obtained by heating the substrate to 625 K under ultrahigh vacuum and turning off the heater current for the approximately 30 s required for LEED acquisition. No changes in either XP or HREEL spectra were detected as a result of the short heating to 625 K.

The O 1*s* 529.4 and 531.2 eV intensities are plotted as a function of O_2 exposure in Figs. 6(a) and 6(b), respectively. The O 1*s* data have been normalized to the Co $2p_{1/2}$ intensity for their particular oxygen exposure to compensate for systematic changes in XPS acquisition among the O_2 annealed surfaces. The 531.2 eV feature, associated with the Co_3O_4-like oxidized surface, saturates after approximately 300 min. Concurrently, the 529.4 eV lattice O^{2-} intensity is attenuated. In order to estimate a minimum thickness for the oxidized layer, we assume that the 531.2 eV O 1*s* species is characteristic of a Co_3O_4-like oxide which forms epitaxially on top of the CoO(100) substrate and we attribute the entire 529.4 eV intensity to the CoO(100) substrate. The solid lines in Fig. 6 follow intensity changes anticipated for a Frank–Van der Merwe growth mode assuming a constant rate of O_2 adsorption,[29] indicating the data are compatible with layer-by-layer epitaxial formation. Attempts to fit the data to Volmer–Weber island growth were unsuccessful.

Calculations of the thickness furthermore assume an exponential attenuation of the XPS photoelectron with a mean free path of 11 Å:[30]

$$\frac{I_{\mathrm{O},1s(\mathrm{Co_3O_4})}}{I_{\mathrm{O},1s(\mathrm{CoO})}}=\frac{S_{\mathrm{O},1s(\mathrm{Co_3O_4})}\int_{n=0}^{m}C_{\mathrm{O},x(\mathrm{Co_3O_4})}\exp(-x\cos\theta/\lambda_{\mathrm{O},1s(\mathrm{Co_3O_4})})dx}{S_{\mathrm{O},1s(\mathrm{CoO})}\int_{n=m+1}^{\infty}C_{\mathrm{O},x(\mathrm{CoO})}\exp(-x\cos\theta/\lambda_{\mathrm{O},1s(\mathrm{CoO})})dx},$$

where m is the thickness of the Co_3O_4 layer, and x is the distance into the surface. S_x are the cross sections of the O 1*s* photoelectron in Co_3O_4 and CoO, respectively, which are assumed to be the same. $C_{O,x(Co_3O_4)}$ and $C_{O,x(CoO)}$ are taken to be constant and equivalent since, in the bulk, both rocksalt CoO and spinel Co_3O_4 are closest packed in lattice oxygen with oxygen–oxygen spacings to within 5%. The spectrometer collection angle, θ, is 42°.

Results of the thickness calculations as a function of oxygen exposure are shown in Fig. 7. The data are given in terms of monolayers, with the average monolayer thickness taken to be 2.13 Å, the distance between layers in the CoO bulk along the ⟨100⟩ direction.[31] The Co_3O_4 epitaxy is only able to grow to a thickness of 5 monolayers (ML), after which the oxidation of the CoO(100) substrate ceases. Admixture of 531.2 and 529.4 eV oxygen species into the CoO substrate and the Co_3O_4-like overlayer would lead to larger calculated thickness values, and thus a 5 ML limiting thickness should be taken as a lower estimate for the CoO(100)–Co_3O_4 epitaxial growth. However, the limiting thickness is comparable to other constrained oxide epitaxies that have been reported to date, e.g., NiO(111) on Ni(100),[32] which form thermodynamically unstable orientations of the oxide and thus do not propagate beyond 3–5 ML.

Assuming bulk termination, the Co_3O_4 orientation that most closely matches the lattice dimensions of the CoO(100) substrate is Co_3O_4(100). Both surfaces have square arrays of oxygen with oxygen–oxygen distances to within 5%. The two surfaces differ primarily in the cobalt ion concentrations and site occupancies. For rocksalt monoxides, the most thermodynamically stable surface orientation is (100), which produces a nonpolar lattice of interpenetrating cation and anion square arrays,[4] effectively balancing out repulsive and maximizing attractive coulombic interactions. In the spinel structure, coulombic interactions are most favorable for (110) and (111) surfaces,[14] which are the naturally occurring orientations observed on flux-grown Co_3O_4 crystals.[33] While less thermodynamically stable, the Co_3O_4(100) orientation preserves the substrate oxygen lattice arrangement. Under sufficiently oxidizing conditions, a Co_3O_4-like oxide will, therefore, form but it is constrained to do so in the (100) orientation in order to interface with the underlying substrate.

The extent to which this Co_3O_4-like oxide layer accurately reflects a true Co_3O_4(100) surface is by necessity a matter of some speculation, since no studies of single-crystal Co_3O_4(100) have been reported. LEED analysis of these thin films indicate the CoO(100) (1×1) symmetry is preserved

throughout the oxidation process, although some streaking is observed along ⟨010⟩ and ⟨001⟩ directions. Since the oxide layer grows to a substantial thickness (≈5 ML) the Co_3O_4-like oxide epitaxy must also preserve the (1×1) unit cell structure. According to XPS data, the cobalt ions are comparable in chemical nature to that of Co_3O_4. Oxygen to cobalt XPS intensities also indicate that the oxide composition is close to that expected for Co_3O_4. However, the oxygen in the Co_3O_4-like layer is substantially different than the O^{2-} of the underlying CoO substrate, or from the majority of the oxide ions in powered Co_3O_4 samples that have been studied by XPS.[21–23]

A simple interpretation of the shift in binding energy from 529.4 eV (CoO 1*s*) to 531.2 eV (oxide overlayer 1*s*) is that the oxygen in the Co_3O_4-like layer is less ionic, and is somewhat closer to O^- than to the O^{2-} of the typical cobalt oxide lattice oxygen. Al_2O_3 and SiO_2 both have formally O^{2-} valent lattice oxygens with binding energies of >531 eV.[27] However, the chemical natures of cations and anions are symbiotic and it is difficult to envision the anion in the oxide overlayer changing without the cations mirroring the change in either their XPS binding energies, anion/cation concentrations, or both. Differences in external relaxation or other final state effects could potentially result in a higher O 1*s* binding energy, but the present data are insufficient to explain the phenomenon. It is clear that the very intense 531.2 eV O 1*s* peak is not a result of either defects or hydroxyl contamination, but is characteristic of the oxide layer that forms on CoO(100) under mild oxidation conditions. The oxide layer is substantial in thickness (≈5 ML) and has enough long-range order to support cooperative vibrational motions to give rise to HREEL phonon spectra.

IV. CONCLUSIONS

At 625 K and under 5×10^{-7} Torr O_2 CoO(100) oxidizes slowly to produce a Co_3O_4-like oxide overlayer. The orientation of bulk Co_3O_4 that best forms an epitaxial arrangement with the underlying CoO(100) substrate is not that which results in a thermodynamically stable Co_3O_4 surface orientation and the epitaxy is limited to approximately 5 ML in thickness. The oxidized overlayer gives a LEED pattern consistent with the underlying substrate CoO(100)–(1×1), but with some streaking along ⟨010⟩ and ⟨001⟩. O 1*s*/Co 2*p* intensities are consistent with the formation of Co_3O_4, as are Co 2*p* binding energies and satellite structure. However, the O 1*s* binding energy associated with the overlayer is 531.2 eV. While the feature has been observed previously on oxidized CoO and Co_3O_4 powders, it is considerably higher in binding energy than the 529.4 eV O 1*s* peak associated with the stoichiometric lattice oxygen. The higher binding energy peak is not a result of water or hydroxyl contamination, since no OH vibrational feature is observed in the HREEL spectrum. The structure of the CoO(100)–Co_3O_4 overlayer must have long-range order, since the LEED is still characteristic of a cubic (1×1) surface. Additionally, phonon structure due to cooperative lattice vibrations is observed in the HREELS, indicating an oxide with a lower unit cell symmetry but significant enough long-range order to support a very well developed Fuchs–Kliewer phonon spectrum.

ACKNOWLEDGMENTS

The authors are grateful for support from NSF under Grant No. CHE9220341 and for partial support under AFOSR Contract No. F49620-94-1-0433.

[1]K. S. Kim, Phys. Rev. B **11**, 2177 (1975).
[2]Z. X. Shen *et al.*, Phys. Rev. B **42**, 1817 (1990).
[3]Z. X. Shen, C. K. Shih, O. Jepsen, W. E. Spicer, I. Lindau, and J. W. Allen, Phys. Rev. Lett. **64**, 2442 (1990).
[4]V. E. Henrich, *Surface and Near-Surface Chemistry of Oxide Materials*, edited by L. C. Dufour and J. Nowotny (Elsevier, New York, 1987), p. 23.
[5]C. N. Satterfield, *Heterogeneous Catalysis in Industrial Practice*, 2nd ed. (McGraw–Hill, New York, 1991), p. 319.
[6]P. Hauptmann, *Sensors: Principles and Applications* (Prentice–Hall, Englewood Cliffs, NJ, 1993).
[7]G. A. Carson, M. H. Nassir, and M. A. Langell, Mater. Res. Soc. Symp. Proc. B **1**, 2.1 (1994).
[8]R. D. Shannon and C. T. Prewitt, Acta Crystallogr. B **25**, 925 (1969).
[9]K. W. Wulser and M. A. Langell, J. Electron Spectrosc. Relat. Phenom. **59**, 223 (1992).
[10]B. L. Klingenberg, F. Grellner, D. Borgmann, and G. Welder, Surf. Sci. **296**, 374 (1993).
[11]J. H. Scofield, J. Electron Spectrosc. Relat. Phenom. **8**, 129 (1976).
[12]C. R. Brundle, T. J. Chuang, and D. W. Rice, Surf. Sci. **59**, 413 (1976).
[13]J. Grimbolt, J. P. Bonnelle, and J. P. Beaufils, J. Electron Spectrosc. Relat. Phenom. **8**, 437 (1976).
[14]B. Marcus-Saubat, J. P. Beaufils, and Y. Barbaux, J. Chim. Phys. **83**, 317 (1986).
[15]M. H. Nassir and M. A. Langell, Solid State Commun. **92**, 791 (1994).
[16]R. Fuchs and K. L. Kliewer, Phys. Rev. A **140**, 2076 (1965).
[17]H. Ibach, Phys. Rev. Lett. **24**, 1416 (1970).
[18]J. Sakurai, W. J. L. Buyers, R. A. Cowley, and G. Dolling, Phys. Rev. **167**, 510 (1968); W. Reichardt, V. Wagner, and W. Kress, J. Phys. C **8**, 3955 (1975).
[19]R. J. Powell and W. E. Spicer, Phys. Rev. B **2**, 2182 (1970).
[20]J. R. Christman, *Fundamentals of Solid State Physics* (Wiley, New York, 1988), p. 299.
[21]C. R. Brundle, T. J. Chuang, and D. W. Rice, Surf. Sci. **60**, 286 (1976).
[22]G. Tyuliev and S. Angelov, Appl. Surf. Sci. **32**, 381 (1988).
[23]M. Oku and Y. Sato, Appl. Surf. Sci. **55**, 37 (1992).
[24]J. van Elp, J. L. Wieland, H. Eskes, P. Kuiper, G. A. Sawatsky, F. M. F. de Groot, and T. S. Turner, Phys. Rev. B **44**, 6090 (1991).
[25]R. B. Moyes and M. W. Roberts, J. Catal. **49**, 216 (1977).
[26]B. W. Lee, A. Ignatiev, J. A. Taylor, and J. W. Rabalais, Solid State Commun. **33**, 1205 (1980).
[27]C. D. Wagner, W. M. Riggs, L. E. Davis, and J. F. Moulder, *Handbook of X-ray Photoelectron Spectroscopy* (Perkin–Elmer, Eden Prairie, MN, 1979).
[28]N. S. McIntyre and M. G. Cook, Analyt. Chem. **47**, 2208 (1975).
[29]R. Kern, G. Lelay, and J. J. Metois, *Current Topics in Material Science*, edited by S. D. Kaldes (North-Holland, Amsterdam, 1979), Vol. 3, Chap. 3.
[30]D. R. Penn, J. Electron Spectrosc. Relat. Phenom. **9**, 29 (1076).
[31]H. E. Swanson, M. I. Cook, T. Isaacs, and E. G. Evans, *Standard X-ray Diffraction Powder Patterns*, Natl. Bur. Stand. C.R S39 (US GPO, Washington, DC, 1990), Vol. 9.
[32]M. A. Langell and M. H. Nassir, J. Phys. Chem. **99**, 4162 (1995).
[33]J. P. S. Badyal, X. Zhang, and R. M. Lambert, Surf. Sci. Lett. **255**, L15 (1990).